

## Original papers

## Automated vision-based system for monitoring Asian citrus psyllid in orchards utilizing artificial intelligence

Victor Partel<sup>a</sup>, Leon Nunes<sup>a</sup>, Phil Stansly<sup>b</sup>, Yiannis Ampatzidis<sup>a,\*</sup><sup>a</sup> Agricultural and Biological Engineering Department, Southwest Florida Research and Education Center, University of Florida, IFAS, 2685 SR 29 North, Immokalee, FL 34142, USA<sup>b</sup> Department of Entomology and Nematology, Southwest Florida Research and Education Center, University of Florida, IFAS, 2685 SR 29 North, Immokalee, FL 34142, USA

## ARTICLE INFO

## ABSTRACT

**Keywords:**  
 Huanglongbing (HLB)  
 Asian citrus psyllid (ACP)  
 Insect detection  
 Machine vision  
 Deep learning  
 Neural networks

Specialty crop growers face challenges from numerous diseases and pests. For example, the Asian citrus psyllid (ACP) is a key pest of citrus due to its role as vector of huanglongbing (HLB) (greening disease). There is no known cure for HLB, but vector management is critical, both for slowing spread and attenuating symptoms in infected trees. Therefore, monitoring ACP population, as well as other pest populations, is an essential management component for timing and assessment of control actions. Manual crop scouting is often labor intensive and time consuming. In this work, an automated system was developed and evaluated utilizing machine vision and artificial intelligence to monitor ACP in groves. This system comprised a tapping mechanism to collect insects from the tree's branches and a board with a grid of cameras for image acquisition. A software was developed using two convolutional neural-networks to accurately detect and distinguish psyllids from other insects and debris fallen from the tree. A GPS was utilized to automatically record individual tree position to facilitate data assessment on large groves. A precision and recall of 80% and 95%, respectively, was obtained on detecting ACPs on a sample of 90 young citrus trees. The system proved a great potential to automate scouting procedures in citrus and to be extended to other crop insects.

## 1. Introduction

The Huanglongbing (HLB), or citrus greening, is a significant disease that affects citrus orchards causing rapid decline of the trees (Chung and Bransky, 2005). HLB was first reported in 1919 in southern China, and it is spread already to 40 different countries all around the world, including the USA (Bové, 2006). The disease causes an immunologic resistance reduction affecting orange production by causing fruit drop and the production of small, misshapen and low-level of juice fruit with no economic value (Hedges and Spreen, 2012; Albrecht and Bowman, 2009). The causal agent of HLB in the America and Asia is usually the *Candidatus Liberibacter asiaticus* (CLas), a phloem limited gram-negative bacterium (Jagoueix et al., 1994; Garnier and Bové, 1996). In 17 years (between 2000 and 2017), the citrus cultivated area in Florida declined 45% and the volume production utilized declined by 71%, mainly due to problems generated by the HLB (Court et al., 2018). Between 2012 and 2017 in Florida, citrus production revenue decreased approximately 47% (from approximately 2.1 billion dollars to approximately 1.2 billion dollars) (Court et al., 2018), resulting in an

average annual reduction of 7945 jobs and \$1.098 billion in industry output (Court et al., 2017).

The HLB is transmitted by the vector *Diaphorina citri* Kuwayama, most know as Asian Citrus Psyllid (ACP) (Hemiptera: Phyllidae). It was verified in Florida for the first time in 1998 (Halbert and Manjunath, 2004). The transmission of the disease occurs in three steps: (i) an initial period of acquisition, when the nymphs and the adults come in contact with the pathogenic agent (CLas), (ii) a latency period, that may include a bacteria reproduction too (Inoue et al., 2009) and (iii) the inoculation period, where the vector transmits the bacteria (presents in the salivary glandules, muscles, tissue and ovaries) to the plant (Ammar et al., 2011; Ammar et al., 2010). The ACP can move about 100 m in 3 days (Boina et al., 2009) and recent data showed a dispersion distance of at least 2 km in 12 days (Lewis-Rosenblum, 2011). This vector exhibits biological characteristics such as high reproduction capacity, fast population growth ratio and capacity to withstand a wide temperature range, which allows it to spread quickly (Halbert and Manjunath, 2004). Bacteria control is becoming virtually unsustainable as robust methods of bacteria elimination are expensive and not effective

\* Corresponding author.

E-mail address: [i.ampatzidis@ufl.edu](mailto:i.ampatzidis@ufl.edu) (Y. Ampatzidis).

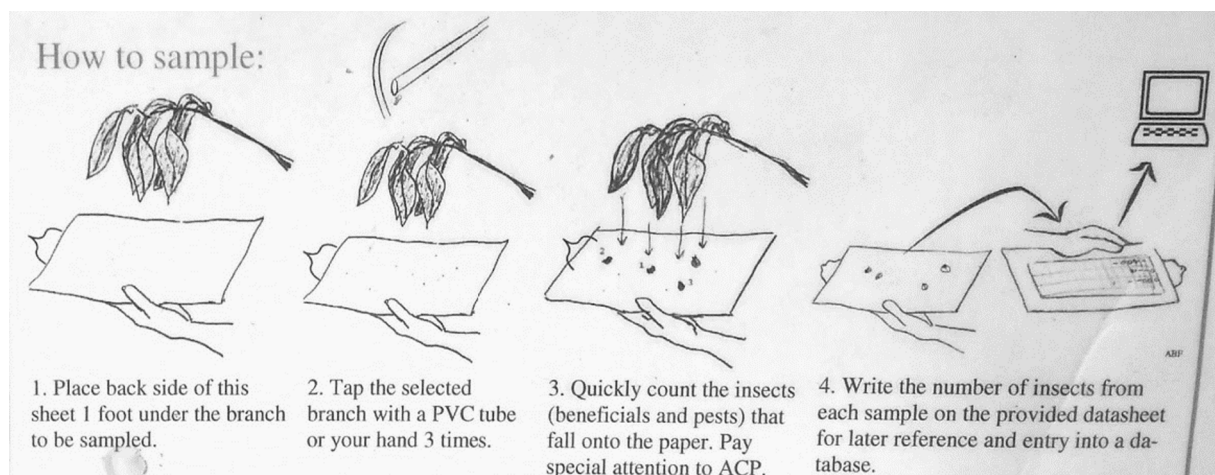


Fig. 1. Traditional (manual) ACP monitoring tap sample method (Arevalo et al., 2012).

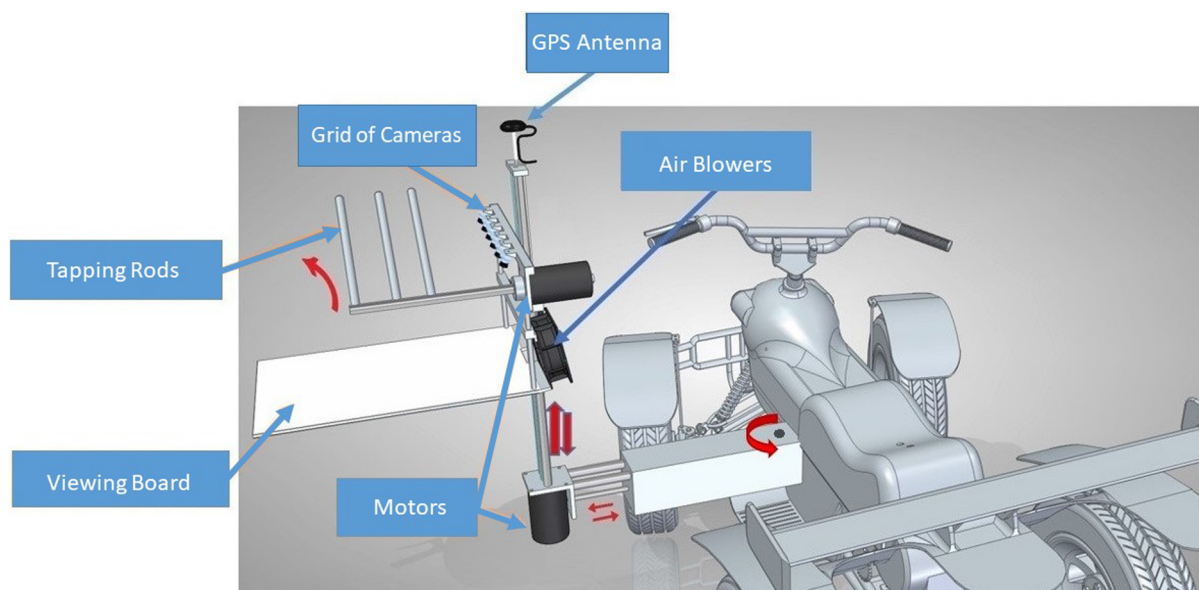


Fig. 2. Example of an initial design for the proposed automated and mobile system for monitoring and mapping pests (e.g. Asian citrus psyllid) in citrus groves (including all moving components of the system).

(Halbert and Manjunath, 2004). Therefore methods for monitoring and controlling the ACP populations are shown to be more advantageous in the prevention and mitigation of the citrus greening problem, allowing the treatment only in critical plants, saving time and reducing costs (Halbert and Manjunath, 2004).

A method to combat the ACP vector includes extensive chemical control programs, by the application of pesticides. However, empirical studies are showing that pesticides application to prevent the introduction and dissemination of ACP has not been very effective (Gottwald, 2007). Besides that, ACP populations have become more resistant to chemicals (Tiwari et al., 2011), which can become problematic without controlled use of pesticides. The use of biological agents as natural predators of the vector is another method of population control (Hall, 2013), in which case chemicals can reduce the effectiveness of the method (Halbert and Manjunath, 2004). Fungi control (entomopathogenic fungi) was also reported as a good tool to control ACP populations (Hall, 2013; Moran et al., 2011; Samson, 1974; Subandiyah, 2000). All the mentioned control methods should be supported by a strong geolocation analysis of ACP quantities, identifying most affected areas and generating accurate targets, both to chemical and biological control of the vector.

Monitoring the ACP population is an essential component of ACP management, both for application of economic thresholds as well as assessing effectiveness of control actions (Monzo and Stansly, 2017). For this purpose, the tap sample method (other traditional ACP monitoring methods are presented below), which requires striking a randomly selected branch and counting ACP falling onto a sheet, has proven to be an efficient and reliable tool for assessing ACP numbers in the tree canopy (Hall and Hentz, 2010; Monzo et al., 2015). Spraying based on need as indicated by tap sample counts has been shown to reduce ACP management costs and conserve natural enemies (Monzo et al., 2014; Monzo and Stansly, 2017). However, this tap sample manual counting method is very labor intensive and time consuming.

Since labor shortage is a major issue in USA, machine vision techniques, internet of things (IoT) (Ampatzidis et al., 2018; Ampatzidis et al., 2012) and cloud-based technologies (Ampatzidis et al., 2016) can simplify pest scouting procedures and improve precision spraying applications (Partel et al., 2019), reduce labor cost, decrease data collection time, and produce critical and practical information (Ampatzidis et al., 2017; Luvisi et al., 2016). Rapid methods for early detection of pests and diseases would assist growers in making timely management decisions and to limit spread (Abdulridha et al., 2019; Abdulridha et al.,

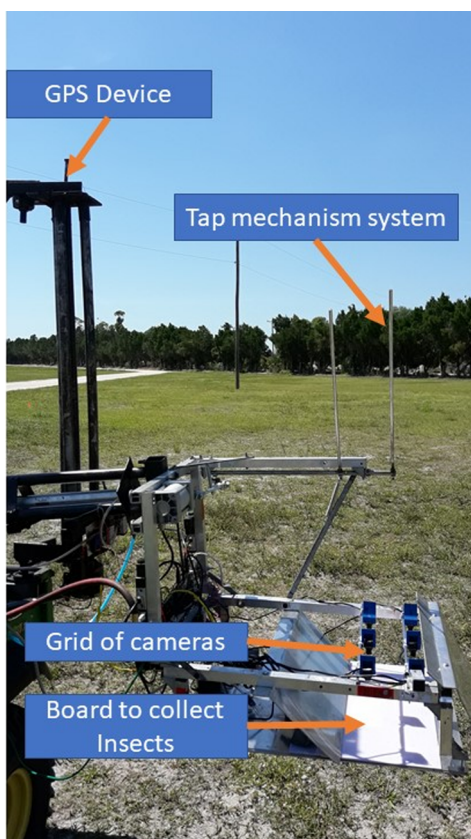


**Fig. 3.** Main hardware components of the automated prototype.

2018).

Machine vision along with artificial intelligence (AI) techniques has been increasingly applied to agriculture (Cruz et al., 2017). Moller (2010) concluded that using computer vision technologies on agricultural operations lowers the operator stress levels (Moller, 2010).

Deep learning based convolutional neural networks (CNN) is the most common AI approach for image recognition and have proven to achieve great performance on image detection and classification tasks (Krizhevsky et al., 2012; Güçlü, 2014; Cruz et al., 2019). Their deep architecture and good weight equalization schemes provide great sensitivity to detect complex and high level features. CNN's have the advantage to be trained from large sets of data, eliminating the need to manually design feature extraction algorithms. In this study, a novel artificial intelligence technology utilizing deep learning was developed and evaluated to automate ACP scouting procedures in citrus orchards, providing rapid and valuable information to improve ACP management.

## 2. Material and methods

### 2.1. Traditional ACP monitoring methods

There are several methods to monitor ACP populations in order to determine the need to spray (Stansly et al., 2010; Hall et al., 2007): (i) the yellow sticky trap which uses an adhesive board to collect psyllids for later visualization; however, sticky traps sampling is slow, labor intensive, costly and assesses ACP in flight, which may not always correlate well with numbers in trees. (ii) Sweep nets, where a net of 15-inch diameter is used into the canopy of trees to collect insects; (iii) the tap sample method which uses a PVC stick to hit the tree's branches forcing the psyllids to fall over a white board positioned bellow to visualize the insects. Other recent technologies as the Spensa Tech® Z-trap® (Spensa Tech, 2018) uses computational machine vision to monitor insects collected on the device fixed in orchards.

The tap sample method is the most common sampling method used nowadays in Florida (Stansly et al., 2010), being a fast and low cost method comparing to others. Tap sampling requires striking a randomly selected branch with a stick or length of PVC pipe and counting ACP adults falling onto a laminated sheet held below (Fig. 1). The tap sample has proved to be a fast and reliable tool for assessing ACP numbers in the tree canopy, and was adopted in 2011 by the United States Department of Agriculture (USDA) Animal Plant Health Inspection Service - Plant Protection and Quarantine (APHIS-PPQ) and the

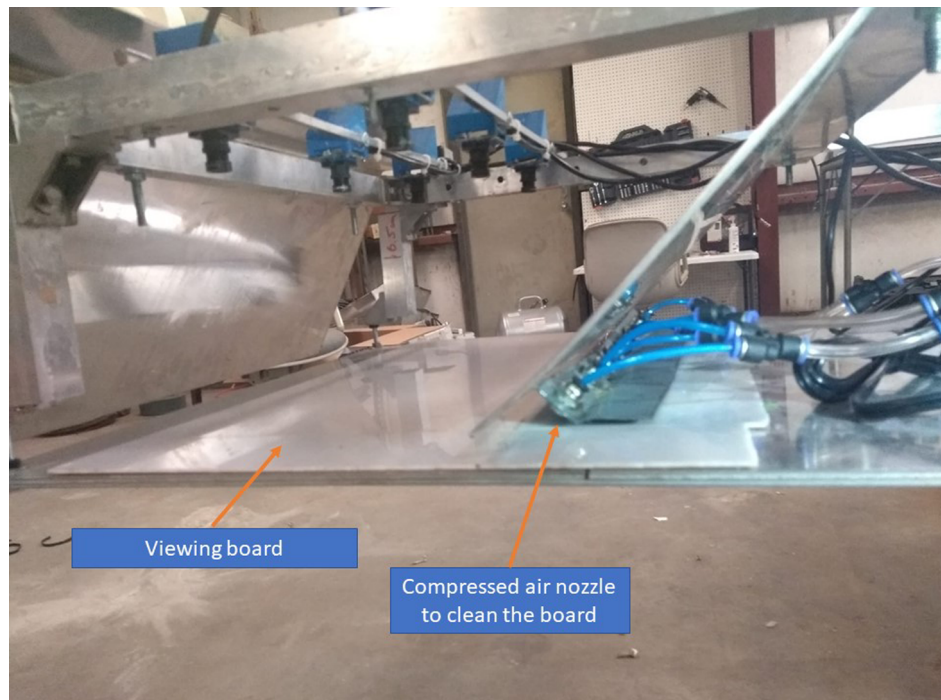


**Fig. 4.** Viewing board with white background and an air blower system to clear the stage after every tree scouting.

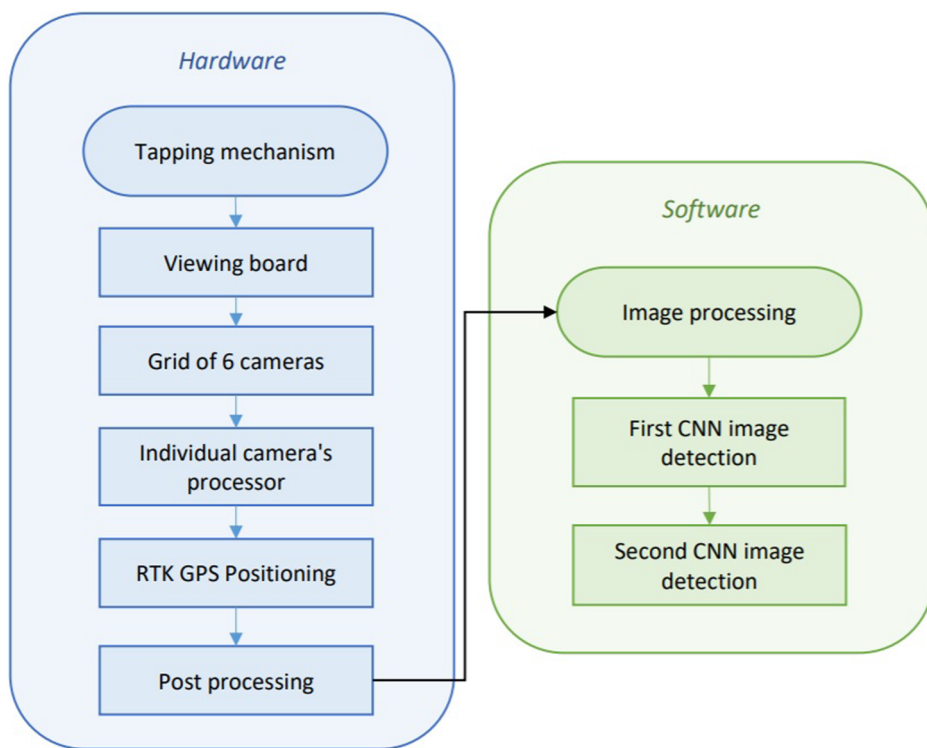


**Fig. 5.** Workflow of hardware and software structures of the prototype.

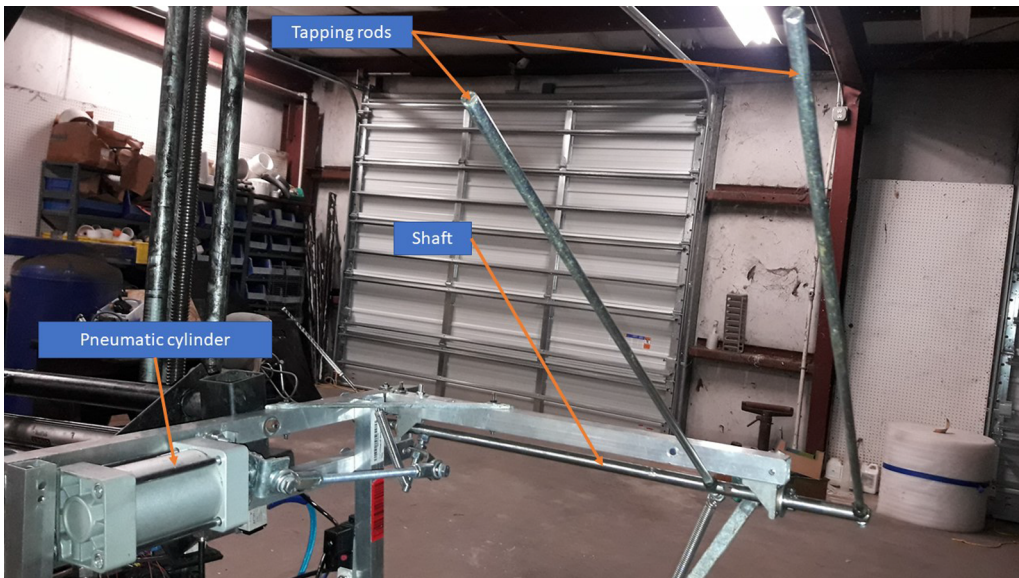


**Fig. 6.** Pneumatic tapping mechanism.

Florida Department of Agriculture and Consumer Services - Division of Plant Industry (FDACS-DPI) as an integral part of the citrus health response program (CHRP). Currently, CHRP employs some 80 workers to monitor over 5000 blocks of citrus every 3 weeks in Florida using the tap sample (Monzo et al., 2015). Results are rapidly made available to clientele by email and on the website [www.flchma.com](http://www.flchma.com).

However, most successful growers supplement this government service with their own ACP monitoring system to provide block by block information needed to fine-tune ACP control (Monzo and Stansly, 2017). Real-time georeferenced ACP incidence data could be used to mitigate spray delivery for development of a precision, target-based sprayer. Automated and georeferenced ACP monitoring is first logical step toward precision ACP management.

## 2.2. Automated system for ACP monitoring

This automated, mobile and intelligence vision-based tap system can rapidly and accurately detect and monitor ACP (and potential other pests and beneficial insects) in the field. Data can be transmitted via the internet to a remote mapping program in real time. This system can be mounted on a mobile vehicle/platform (e.g. all-terrain vehicle, ATV; Fig. 2).

The proposed technology comprised hardware and software components. The hardware (Fig. 3) includes: (i) a tapping mechanism to struck the tree's branches so that ACPs fall; (ii) a viewing white board located below the tapping mechanism to collect the fallen ACPs for observation; (iii) a grid of high resolution cameras to acquire images of

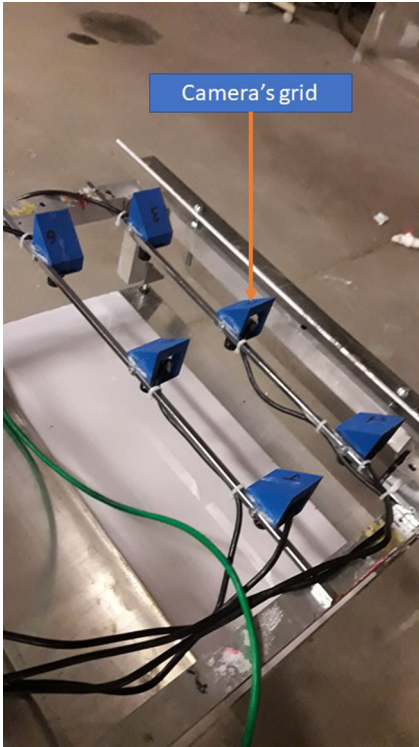


Fig. 7. Grid of six cameras positioned above viewing board.

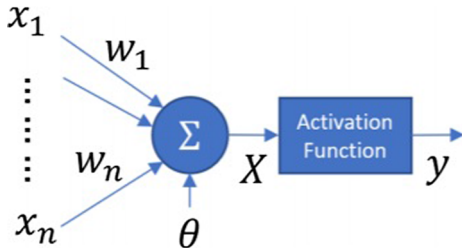


Fig. 8. Representation of a single neuron on a neural network. A neuron receives inputs  $x$  and holds weights  $w$ ;  $\theta$  is the bias term. The resulting element  $X$  is the dot product of  $x$  and  $w$  plus the bias term. It is thresholded by the activation function to produce the output  $y$ .

the board right after the tapping; (iv) camera's processor units to individually control each camera's image acquisition; (v) and a real-time kinematic Global Positioning System (RTK-GPS) to geolocate each tree and ACPs detection. The software developed to perform the post processing image detection includes: (a) an image processing method; (b) a first convolutional neural network (CNN) object detection; and (c) a second CNN detection in order to accurately distinguish ACPs on images. The prototype was designed to be low cost and use accessible components, adding a total of less than \$2000.

The automated ACP detection procedure includes the following steps: (1) the operator places the system next to a tree branch. There are three movable axes for better positioning the system in a tree (Fig. 2): (i) up & down; (ii) front and back; and (iii) rotational movement. (2) The “striking paddles” of the shaking system agitates the tree branches. (3) An array (grid) of cameras to collects pictures. (4) The air blower system removes all the material from the “viewing stage” (Fig. 4). (5) The smart controller analyzes the images, detects, geolocates and counts ACP. (6) The unit moves to the next tree. A variable rate sprayer could be mounted at the front of a unit for real-time applications varying the amount of agro-chemical as a function of pest density. The work flow of this system is presented in Fig. 5.

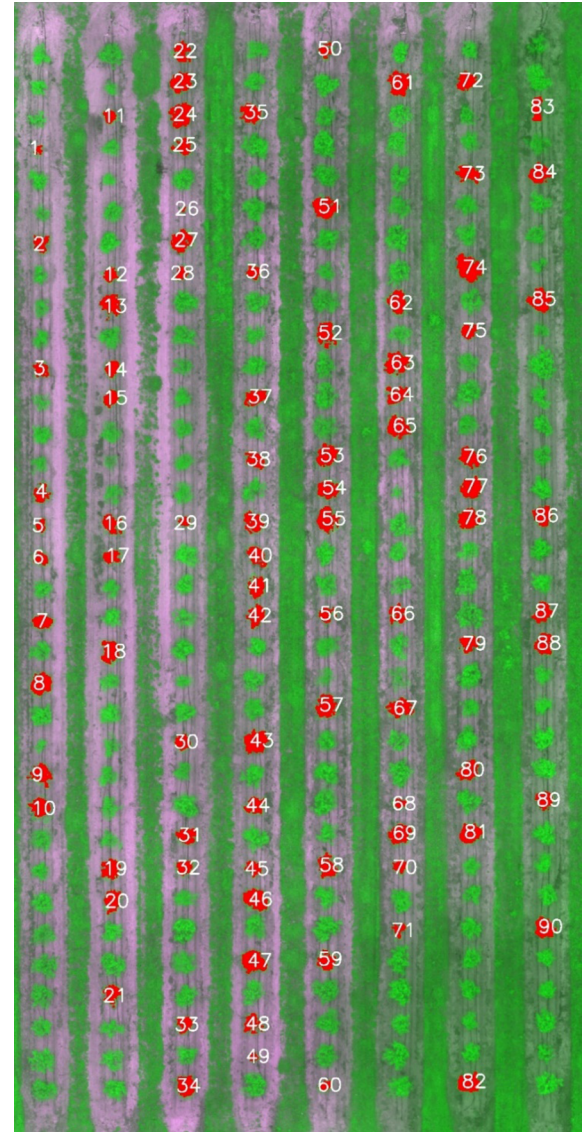


Fig. 9. Aerial map of each randomly selected tree's ID (presented in Table 1) position generated by using the RTK GPS data. For better visualization, scouted tree's canopies were segmented in red using UAV's NDVI values as described by Ampatzidis and Partel (2019). (For interpretation of the references to color in this figure legend, the reader is referred to the web version of this article.)

### 2.2.1. Tapping mechanism

A mechanism was developed to perform a fast and consistent tapping on tree's branches. A pneumatic cylinder (Baomain Electric SC63X50, Yueqing City, China) with a stroke of 50 mm (2 in.) and 63.5 mm (2.5 in.) bore was used to turn a shaft connected to two steel tapping rods of 8 mm diameter and 0.6 m length (Fig. 6). The rods have a stroke of 80 degrees and were measured to achieve a speed of 8 m/s on their ends during the tapping procedure.

### 2.2.2. Viewing board

An acrylic opaque white board with dimensions  $0.45 \times 0.22$  m was used to collect the fallen ACPs for visualization (Fig. 4). The board was chosen to be easy to clean and to reduce reflectance effects.

### 2.2.3. Grid of cameras

For the image acquisition task, a grid of six high resolution USB cameras was used. The cameras were placed so that each camera would cover a  $0.15 \times 0.11$  m area of the viewing board (Fig. 7). The camera module utilized (Spinel UC80MPA\_ND, Irvine, CA, USA) has 8



**Fig. 10.** Prototype positioned to scout a citrus tree and its main components.

megapixels of resolution ( $3264 \times 2448$ ) and a lens of 3.6 mm focal length. The grid was placed 0.14 m above the viewing board. The cameras were configured to acquire one channel images (greyscale) to reduce image processing operations, as there was no relevant color information on one psyllid for the utilized resolution.

#### 2.2.4. Camera's processor

In order to capture images at the same time in all six cameras (within a 0.3 s tolerance), an individual processor unit was used in each camera module to control the image acquisition. The processors used were the Raspberry Pi v3 (Model B, Raspberry Pi Foundation, Cambridge, UK), connected to each respective camera through a USB cable. All the processors were connected to each other through general-purpose input/output (GPIO) pins to trigger them at the same time. One of the processors was also connected to the pneumatic cylinder valve (to control the valve).

A software was created on the processors to trigger the tapping mechanism two times within 0.5 s and then to trigger the image acquisition 0.5 s after the second tap. This delay was found to be suitable after trial-and-error tests as it is enough time for the insects to fall on the board, but it is not long enough so that insects start to fly away. It is important to have a consistent and fast tapping as the ACPs fly off the viewing board only seconds after falling.

#### 2.2.5. RTK GPS positioning

A real-time kinematic (RTK) GPS device (TOPCON HiperXT, Tokyo, Japan) was utilized on the prototype to provide position coordinates of each scouted tree. The device positioning accuracy is around 0.02 m, which was more than enough to locate and distinguish between trees. The developed software integrated the GPS location and the ACPs detection results to automatically generate maps of the scouted area results.

#### 2.3. ACP detection software

After the image collections in the field, the acquired images were sent to an NVIDIA Jetson TX2 embedded computational unit (NVIDIA TX2 Developer Kit, Santa Clara, CA, USA) to be processed on a

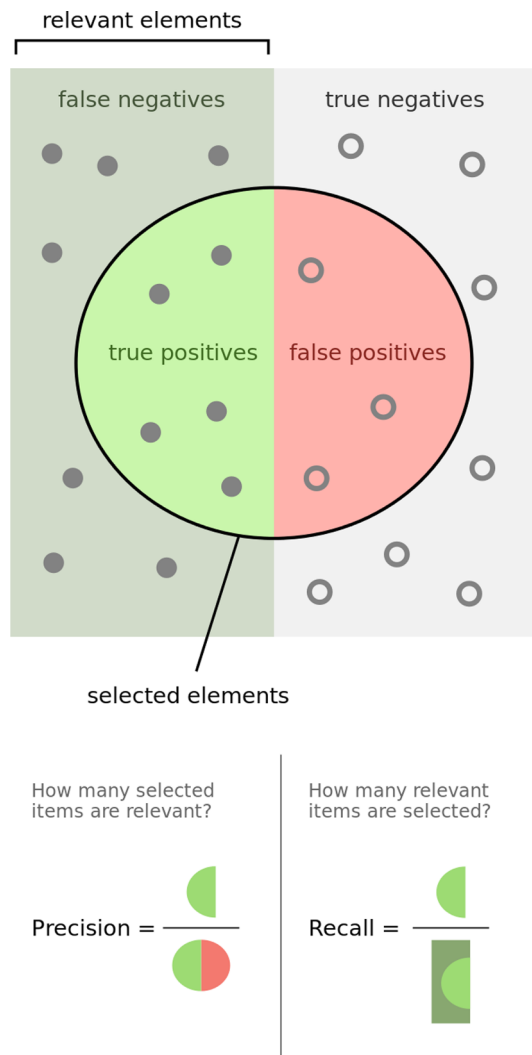


**Fig. 11.** Precision and Recall explained in a graphical format (Wikipedia).

developed software. The software was developed in C to be a fully automated process. First the six images (one image per camera) are merged together to form a full picture of the viewing stage with resolution of  $9792 \times 4896$  pixels. The ACP detection process is divided in two stages of image detection using deep convolutional neural networks.

A neural network consists of many ordered layers of neurons. The input signals are propagated sequentially from the first layer to the end layer of the network to produce an output result. Each neuron contains a weight values vector  $\vec{w}$  that is used to process the input stimulus  $\vec{x}$  and a bias term  $\theta$  that will add to the operation to produce its output as described by Eq. (1) and Fig. 8. The first layer of the network receives the three-dimensional matrix representation of the input image and the end layer output the confidence value of the membership of a sample into a particular population.

$$X = x_1 w_1 + \dots + x_n w_n + \theta \quad (1)$$

CNNs are optimized networks for image recognition tasks. Generally, a CNN will train itself to apply multiple filters on an input image to try to extract relevant features (e.g. traces, shapes) for the classification. The output matrices of the filters are multiplied to be propagated on the network. The multiplication of two matrices is known as convolution, hence the name convolutional neural networks.

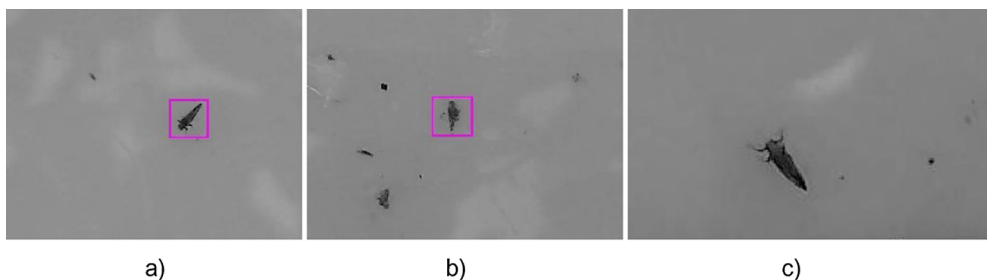


**Fig. 12.** Example of: (a) true positive detection (correct ACP detection); (b) false positive detection (incorrect ACP detection; another object was detected as an ACP); and (c) false negative detection (ACP not detected by the software).

**Table 1**  
ACP detection results from 90 randomly selected citrus trees.

Tree	False positives	False negatives	Detections	Tree	False positives	False negatives	Detections	Tree	False positives	False negatives	Detections	
1	0	0	1	31	1	0	5	61	0	0	4	
2	0	0	2	32	1	0	2	62	0	0	6	
3	2	0	4	33	1	0	3	63	0	0	2	
4	2	0	5	34	1	0	5	64	0	0	3	
5	0	0	3	35	3	0	4	65	0	0	2	
6	0	0	2	36	2	0	4	66	1	0	9	
7	2	1	4	37	1	0	2	67	0	0	8	
8	0	1	1	38	1	1	2	68	1	0	12	
9	0	1	2	39	1	1	2	69	2	0	6	
10	0	0	2	40	1	0	3	70	2	0	6	
11	1	0	1	41	1	0	3	71	0	0	6	
12	1	0	1	42	0	0	1	72	0	0	3	
13	1	0	1	43	1	0	5	73	1	0	1	
14	2	0	2	44	0	0	2	74	0	0	3	
15	1	0	3	45	0	0	2	75	0	0	1	
16	1	0	3	46	0	1	1	76	0	0	5	
17	1	0	1	47	1	0	9	77	0	1	5	
18	0	0	1	48	2	0	13	78	3	0	4	
19	0	1	1	49	0	0	4	79	0	0	2	
20	0	0	1	50	1	1	5	80	0	0	3	
21	1	1	2	51	2	0	7	81	0	0	2	
22	0	0	1	52	0	0	3	82	0	0	0	
23	1	0	2	53	1	0	4	83	1	0	3	
24	2	0	3	54	1	0	6	84	1	0	3	
25	1	0	2	55	0	0	1	85	0	1	2	
26	1	0	3	56	2	0	15	86	0	0	1	
27	1	0	6	57	2	0	14	87	1	0	4	
28	3	1	6	58	0	0	6	88	0	0	5	
29	2	1	5	59	0	0	5	89	1	0	4	
30	1	1	4	60	0	0	4	90	1	0	4	
Total	Detections	336		True positives	267			False positives	69		False negatives	14

### 2.3.1. First CNN ACP detection

A first deep learning convolutional neural network was trained using YOLOv3 (You Only Look Once), a state-of-the-art object detection system (Redmon and Farhadi, 2018). YOLOv3 is a single-stage method for object detection consisting of 106 fully connected neural layers. A training set of 800 labeled images was prepared by capturing images of ACPs on a white background. The network was trained for 10,000 iterations using a common learning rate of 0.01.

The first CNN was found to be fast and sensitive to predict and locate possible ACP objects, but it was not very accurate in doing so. In other words, it showed a great performance on recall (sensitivity) but not on precision (accuracy). For this reason, the first CNN was used to predict all possible ACP objects position to be later filtered by a second fine-tuned CNN. An empirical threshold of 0.001 was utilized on this first CNN object detection.

### 2.3.2. Second CNN ACP detection

After obtaining the possible ACP objects position from the first CNN detection, each object is cropped into a  $64 \times 64$  pixels image, which was found to be an ideal image size to contain an individual adult ACP. The cropped images are then normalized to reduce light variance effects on the grid.

A second CNN was trained using YOLOv1, which is a previous version of YOLOv3 that has 24 convolutional layers instead of 106 on

the newer version. The smaller network was empirically found to be more suited for the image classification on  $64 \times 64$  pixels resolution. This observation is possibly explained by the fact that the 106 layers network has too many weight's variables to be configured for a  $64 \times 64$  input image classification, generating overfitting. A training set was collected and labeled of around 8000  $64 \times 64$  pixel's images including individual ACP as well as other collected insect and debris from tree's branches on a white background. The network was trained for 4000 iterations using a learning rate of 0.001, empirical values that were found to reduce overfitting. An empirical detection threshold of 0.4 was used to classify the images into ACP or other (e.g. debris).

### 3. Experimental design

All the tests were performed at the University of Florida's Southwest Florida Research and Education Center (SWFREC) located in Immokalee, Florida, USA. The grove used to evaluate the developed technology contains 8 rows of 80 m length with two different citrus varieties, Valencia and Swingle citrumelo, being 18 months old at the date of the experiment. The prototype was attached to an ATV (John Deere Gator™) to move it around the field. All the data were collected on February 13th of 2019, between 10:00 am to 12:00 pm.

The experiment was conducted by randomly selecting 90 trees between the 8 rows of the field (Fig. 9). Previously, an unmanned aerial

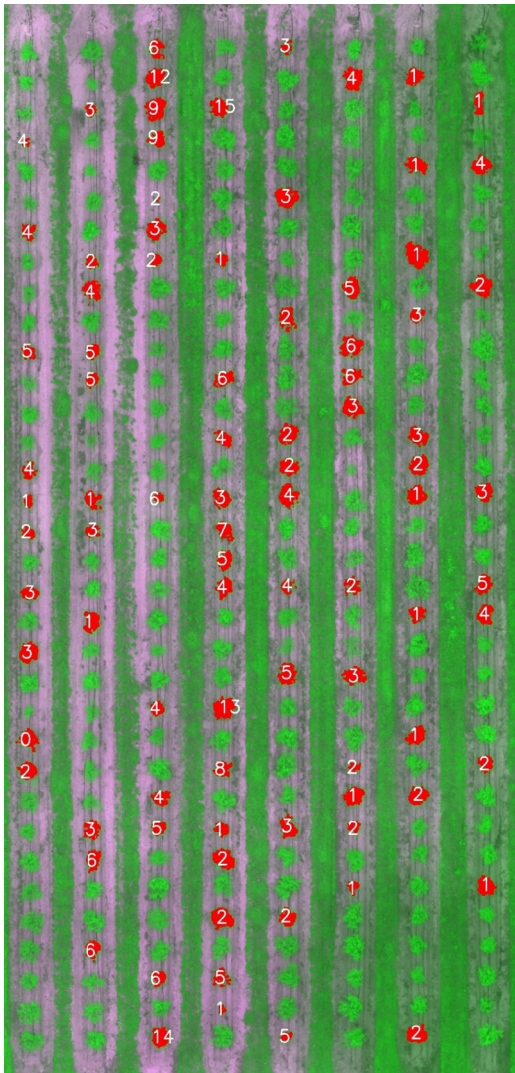


**Fig. 13.** Visualization of ACP detection results (one scouting per tree) on an aerial map for each randomly selected tree. Segments in red were used to measure each tree canopy size. (For interpretation of the references to color in this figure legend, the reader is referred to the web version of this article.)

vehicle (UAV) (DJI Matrice 600, DJI, Shenzhen, China) equipped with a multispectral camera (RedEdge-M, MicaSense, Seattle, WA) was used to fly above the study area and obtain an aerial picture for better visualization of the collected ACP data. A vision-based technique was utilized to automatically detect all trees and measure their canopy size as described by Ampatzidis and Partel (2019). Fig. 9 shows the aerial map with the ID of each scouted tree (canopy represented in red). For each analyzed tree the ATV was parked on its side to perform the scouting. The developed technology was then activated to perform the tree's branch tapping and image acquisition (Fig. 10). The images were later processed using the CNNs to detect the ACPs.

To evaluate the performance of the detections each detected image was carefully examined through morphological observations to account for true positives, false positives and false negatives to calculate precision and recall (Fig. 11). Fig. 12 presents an example of: (i) true positive, correct ACP detection (Fig. 12a), (ii) false positive, incorrect ACP detection (e.g. branch debris) (Fig. 12b) and (iii) false negative, incorrect ACP rejection (Fig. 12c). Furthermore, the f-score (harmonic mean of precision and recall) was used to evaluate the ACP detection accuracy too.

#### 4. Results and discussion

The results for the experiment on the 90 trees are shown in Table 1. A total of 267 true positive detections were counted, 69 false positives and 14 false negatives, which result in a precision and recall of 80% and 95%, respectively. The overall f-score result was 87%. The results show that the software performed better on ACPs sensitivity (only 14 missed psyllids) than on accuracy (69 debris misidentified as ACPs), which shows that it was easier to detect ACPs than to distinguish an ACP from some similar shaped debris (or insects). The results accounted for adult ACPs only, ACP nymphs were not noted.

The results data shows a high variance between trees, from 0 to 15 ACPs, which can be explained by the fact that some trees were starting to flush at the experiment date and ACPs would concentrate more in these trees. The actual observed number of ACPs was 281, with an average of 3.1 ACPs per tree. On a different experiment, Hall and Hentz (2010) reported an average of 1.2 ACPs per tree (using the manual tapping method). Many factors are involved in the occurrence of ACPs (per tree) such as the tree location, weather conditions and tree growing stage (e.g. leaf flushing). Other factors that can explain the higher number of ACPs detected by the developed automated system are: (i) the viewing board is 60% larger than a letter-size paper sheet used in a manual tap method procedure, and (ii) the pneumatic tapping mechanism hits the tree branch stronger than the conventional tap which can also vary between individuals. The traditional tap method has been reported to be difficult to measure on large amount of ACPs per branch, as they fly off the pan shortly after falling (Hall and Hentz, 2010).

Most of the misidentified ACPs were found to be small pieces of debris with a similar shape and size, which was challenging to distinguish on the utilized resolution even for a non-trained observer. Two main limitations were observed regarding the image acquisition, resolution and focus. Higher resolution images could help distinguish better ACP characteristics from debris, although the 48 megapixels resolution of the grid is already fairly high, providing an average 60x60 pixels resolution for an adult psyllid. The camera focus was also found to be a limitation factor for a clearer image acquisition. As each camera's viewing area has a different distance to the lens (higher distance on corners of viewing area and shorter on the center); this produces differences in focus for each area. A possible solution for this would be increase the camera's height as it would reduce differences on the grid depth.

##### 4.1. ACP geo-location

The position coordinates obtained from the RTK-GPS were saved for each tree at the moment of the scouting (in real-time). These data were used to create a map of the scouted trees in the field. Fig. 13 presents the detection ACP numbers for every randomly selected tree in this map. It has to be noted that each tree was assessed on a single branch, thus the detection results can be used as an estimate (the actual ACP population per tree might be higher). Multiple scouting on different branches of each tree can be done for a better estimation of the insect population per tree. The canopy size of each tree (developed based on Ampatzidis and Partel, 2019) can be further used to investigate any correlations with ACP detections etc., which is out of the scope of this paper.

#### 5. Conclusion and future work

A cost-effective automated system to detect, distinguish, count and geo-locate Asian citrus psyllid (ACP) in a citrus grove utilizing machine vision and artificial intelligence was developed and evaluated. This novel technology was designed to automate the conventional stem tap method for ACP scouting. It comprises a tapping mechanism to hit the tree's branches so that insects fall over a board with a grid of cameras used for image acquisition. An NVIDIA TX2 embedded computational unit was used to integrate the software with the hardware. A software was developed using two convolutional neural networks to detect and

distinguish ACPs from other insects and debris, integrated with a GPS device to record position data for each tree and ACPs detection. Results obtained from 90 trees in a citrus grove showed a precision and recall of 80% and 95%, respectively, on distinguishing ACPs from other debris materials. Future studies will compare the proposed technology and methodology with other conventional ACP monitoring methods, as very few data are available as of now on this regard.

A map of scouted trees data was developed using the prototype for better visualization of the collected ACP detection data. This technology shows a great potential on increasing accuracy and reducing labor costs on insect scouting procedures as diseases, like the HLB, continues to impose serious threats to citrus groves all over the world. The proposed technology could benefit growers with more rapid and efficient monitoring of the Asian citrus psyllid populations in the tree canopy and therefore more effective management of this pest.

Future studies will be conducted on extending the technology for other crops and insects. Furthermore, a software will be developed to use the collected ACP detection data and generate prescription maps compatible with precision equipment for variable rate application in order to apply the right amount of pesticides only where needed, and hence, decrease agro-chemical use and expenses, and reduce environmental impact. Spraying costs in Florida citrus where ACP is endemic (Citrus Health Management Areas, CHMA) were estimated at \$727 per acre which is 44.8% of total cultural controls without tree replacement (Singerman, 2018). Of these costs, insecticides (including CHMA sprays) are estimated at \$275 per acre plus \$115 for application. A 25% reduction insecticide and application costs would save \$98 per acre or 6% of the cultural control costs which could make the difference between profit and loss.

## Appendix A. Supplementary material

Supplementary data to this article can be found online at <https://doi.org/10.1016/j.compag.2019.04.022>.

## References

- Abdulridha, J., Ampatzidis, Y., Ehsani, R., de Castro, A., 2018. Evaluating the performance of spectral features and multivariate analysis tools to detect laurel wilt disease and nutritional deficiency in avocado. *Comput. Electron. Agric.* 155, 203–211.
- Abdulridha, J., Ehsani, R., Abd-Erlahman, A., Ampatzidis, Y., 2019. A remote sensing technique for detecting laurel wilt disease in avocado in presence of other biotic and abiotic stresses. *Comput. Electron. Agric.* 156, 549–557.
- Albrecht, U., Bowman, K.D., 2009. *Candidatus Liberibacter asiaticus* and huanglongbing effects on citrus seeds and seedlings. *Horticul. Sci.* 44, 1967–1973.
- Ammar, E.-D., Shatters Jr, R.G., Lynch, C., Hall, D.G., 2011. Detection and relative titer of *Candidatus Liberibacter asiaticus* in the salivary glands and alimentary canal of *Diaphorina citri* (Hemiptera: Psyllidae) vector of citrus huanglongbing disease. *Ann. Entomol. Soc. Am.* 104, 526–533.
- Ammar, E.-D., Shatters Jr, R.G., Lynch, C., Hall, D.G., 2010. Localization of *Candidatus Liberibacter asiaticus*, associated with citrus huanglongbing disease, in its psyllid vector using fluorescence *in situ* hybridization. *J. Phytopathol.* 159, 726–734.
- Ampatzidis, Y., de Bellis, L., Luvisi, A., 2017. iPathology: robotic applications and management of plants and plant diseases. *Sustainability* 9 (6), 1010. <https://doi.org/10.3390/su9061010>.
- Ampatzidis, Y.G., Kiner, J., Abdolee, R., Ferguson, L., 2018. Voice-Controlled and Wireless Solid Set Canopy Delivery (VCW-SSCD) System for Mist-Cooling. *Sustain. Spec. Issue: Inform. Commun. Technol. (ICT) Sustain.* 10 (2), 421. <https://doi.org/10.3390/su10020421>.
- Ampatzidis, Y., Partel, V., 2019. UAV-based high throughput phenotyping in citrus utilizing multispectral imaging and artificial intelligence. *Remote Sens.* 11 (4), 410. <https://doi.org/10.3390/rs11040410>.
- Ampatzidis, Y., Whiting, M.D., Scharf, P.A., Zhang, Q., 2012. Development and evaluation of a novel system for monitoring harvest labor efficiency. *Comput. Electron. Agric.* 88, 85–94.
- Ampatzidis, Y., Wortman, R., Tan, L., Whiting, M., 2016. Cloud-based harvest management information system for hand-harvested specialty crops. *Comput. Electron. Agric.* 122, 161–167.
- Arevalo, H.A., Stansly, P.A., Fraulo, A., Qureshi, J., Buss, L.J., 2012. Tap Sampling for Asian Citrus Psyllid (ACP) Field Sheet. SWFREC – IFAS, Immokalee, Florida, USA.
- Boina, D.R., Meyer, W.L., Onagbola, E.O., Stelinski, L.L., 2009. Quantifying dispersal of *Diaphorina citri* (Hemiptera: Psyllidae) by immunomarking and potential impact of unmanaged groves on commercial citrus management. *Environ. Entomol.* 38, 1250–1258.
- Bové, J.M., 2006. Huanglongbing: A destructive, newly-emerging, century-old disease of citrus. *Plant Pathol.* 88, 7–37.
- Chung, K.R., Bransky, R.H., 2005. Citrus Diseases Exotic to Florida: Huanglongbing (CitrusGreening). Plant Pathology Department Fact Sheet PP-210, Florida Cooperative Extension Service, Institute of Food and Agricultural Sciences, University of Florida. <http://edis.ifas.ufl.edu/PP133>.
- Court, C.D., Hodges, A.W., Rahmani, M., Spreen, T.H., 2017. Economic Contributions of the Florida Citrus Industry in 2015–16. Food and Resource Economics Department, Gainesville, Florida <https://fred.ifas.ufl.edu/media/fredifasufledu/photos/economic-impact/Economic-Impacts-of-the-Florida-Citrus-Industry-2015-16.pdf>.
- Court, C.D., Hodges, A.W., Stair, C., Rahmani, M., 2018. Economic Contributions of the Florida Citrus Industry in 2016–17. Food and Resource Economics Department Gainesville, Florida.
- Cruz, A.C., Ampatzidis, Y., Pierro, R., Materazzi, A., Panattoni, A., de Bellis, L., Luvisi, A., 2019. Detection of Grapevine Yellows Symptoms in *Vitis vinifera* L. with Artificial Intelligence. *Comput. Electron. Agric.* 157, 63–76.
- Cruz, A.C., Luvisi, A., De Bellis, L., Ampatzidis, Y., 2017. X-FIDO: an effective application for detecting olive quick decline syndrome with novel deep learning methods. *Front. Plant Sci.* 10. <https://doi.org/10.3389/fpls.2017.01741>.
- Garnier, M., Bové, J.M., 1996. Distributions of the Huanglongbing (Greening) *Liberobacter* Species in Fifteen African and Asian Countries. IOCIV, Riverside, pp. 388–391.
- Gottwald, T.R., 2007. Citrus canker and citrus huanglongbing, two exotic bacterial diseases threatening the citrus industries of the Western Hemisphere. *Outlooks on Pest Manage.* 18 (274), 279.
- Güçlü, U., Van, G.M.A., 2014. Deep neural networks reveal a gradient in the complexity of neural representations across the brain's ventral visual pathway. *arXiv preprint arXiv:1411.6422*.
- Halbert, S.E., Manjunath, K.L., 2004. Asian citrus psyllids (*Sternorrhyncha: Psyllidae*) and greening disease of citrus: a literature review and assessment of risk in Florida. *Florida Entomol.* 87, 330–353.
- Hall, D.G., Hentz, M.G., Ciomperlik, M.A., 2007. A comparison of traps and stem tap sampling for monitoring adult Asian citrus psyllid (Hemiptera: Phylidae) in citrus. *Fla. Entomol.* 90, 327–334.
- Hall, D.G., Hentz, M.G., 2010. Sticky Trap and Stem-Tap Sampling Protocols for the Asian Citrus Psyllid (Hemiptera: Psyllidae). *J. Econ. Entomol.* 103, 541–549.
- Hall, D.G., Richardson, M.L., Ammar, E.-D., Halbert, S.E., 2013. Asian citrus psyllid, *Diaphorina citri*, vector of citrus huanglongbing disease. *Entomol. Exp. Appl.* 146 (2013), 207–223.
- Hodges, A.W., Spreen, T.H., 2012. Economic Impacts of Citrus Greening (HLB) in Florida, 2006/07–2010/11. University of Florida, Institute of Food and Agricultural Science, Gainesville, FL, USA EDIS document FE903.
- Inoue, H., Ohnishi, J., Ito, T., Tomimura, K., Miyara, S., Iwanami, T., Ashihara, W., 2009. Enhanced proliferation and efficient transmission of *Candidatus Liberibacter asiaticus* by adult *Diaphorina citri* after acquisition feeding in the nymphal stage. *Ann. Appl. Biol.* 155, 29–36.
- Jagoueix, S., Bové, J.M., Garnier, M., 1994. The Phloem-Limited Bacterium of Greening Disease of Citrus Is a Member of the alpha-subdivision of the Proteobacteria. *Int. J. Syst. Bacteriol.* 44, 379–386.
- Krizhevsky, A., Sutskever, I., Hinton, G.E., 2012. ImageNet Classification with Deep Convolutional Neural Networks. In: Proc. Advances in Neural Information Processing Systems 25, pp. 1090–1098.
- Lewis-Rosenblum, H., 2011. Seasonal and long-range movement of Asian citrus psyllid, *Diaphorina citri*. MS thesis. Univ Florida, Gainesville, pp. 75.
- Luvisi, A., Ampatzidis, Y., de Bellis, L., 2016. Plant pathology and information technology: opportunity and uncertainty in pest management. *Sustainability* 8 (8), 831. <https://doi.org/10.3390/su8080831>.
- Moller, J., 2010. Computer vision a versatile technology in automation of agricultural machinery. In: 21st. Annual Meeting, Bologna, EIMA International, Nov 13–14, 2010.
- Monzo, C., Arevalo, H.A., Jones, M.M., Vanaclocha, P., Croxton, V., Qureshi, J.A., Stansly, P.A., 2015. Sampling methods for detection and monitoring of the Asian citrus psyllid (Hemiptera: Psyllidae). *Environ. Entomol.* 1–9. <https://doi.org/10.1093/ee/nvv032>.
- Monzo, C., Qureshi, J.A., Stansly, P.A., 2014. Insecticide sprays, natural enemy assemblages and predation on Asian citrus psyllid, *Diaphorina citri* (Hemiptera: Psyllidae). *Bull. Entomol. Res.* <https://doi.org/10.1017/S0007485314000315>.
- Monzo, C., Stansly, P.A., 2017. Economic injury levels for Asian citrus psyllid control in process oranges from mature trees with high incidence of huanglongbing. *PLoS one* 12 (4).
- Moran, P.J., Patt, J.M., Cabanillas, H.E., Adamczyk Jr, J.A., Jackson, M.A., Dunlap, Christopher A., Hunter, Wayne B., Avery, Pasco B., 2011. Localized autoinoculation and dissemination of *Isaria fumosorosea* for control of the Asian citrus psyllid in South Texas. *Subtropical Plant Sci.* 63, 23–35.
- Partel, V., Kakarla, S.C., Ampatzidis, Y., 2019. Development and evaluation of a low-cost and smart technology for precision weed management utilizing artificial intelligence. *Comput. Electron. Agric.* 157, 339–350.
- Tiwari, S., Mann, R.S., Rogers, M.E., Stelinski, L.L., 2011. Insecticide resistance in field populations of Asian citrus psyllid in Florida. *Pest Manage. Sci.* 67, 1258–1268.
- Redmon, J., Farhadi, A., 2018. Yolov3: An incremental improvement. *arXiv 2018*, arXiv:1804.02767.
- Samson, R.A., 1974. *Paecilomyces* and some allied *Hyphomycetes*. *Stud. Mycol.* 6, 1–119.
- Singerman, A., 2018. Cost of Production for Processed Oranges in Southwest Florida, 2016/17. Food and Resource Economics Department, UF/IFAS Extension, FE1038, <http://edis.ifas.ufl.edu/pdffiles/FE/FE103800.pdf>.
- Spensa Tech, 2018. Z-Trap, [https://www.dtn.com/wpcontent/uploads/2018/07/ss\\_dtn\\_smart\\_trap\\_1018.pdf](https://www.dtn.com/wpcontent/uploads/2018/07/ss_dtn_smart_trap_1018.pdf).
- Stansly, P.A., Arevalo, H.A., Qureshi, J., 2010. Monitoring methods for Asian citrus psyllid. *Citrus Ind.* 91, 20–22.
- Subandiyah, S., Nkoh, N., Sato, H., Wagiman, F., Tsuyumyu, S., Fukatsu, T., 2000. Isolation and characterization of two entomopathogenic fungi attacking *Diaphorina citri* (Homoptera, Psylloidea) in Indonesia. *Mycoscience* 41, 509–513.